A new high-pressure recycle-flow calorimeter and results of determinations with ethane

T. MIYAZAKI,[a] A. V. HEJMADI, and J. E. POWERS

*Department of Chemical Engineering,
The University of Michigan,
Ann Arbor, Michigan 48109, U.S.A.*

A new recycle-flow calorimeter is described with which the thermodynamic properties of fluids can be determined between pressures of 2 to 20 MPa and temperatures of 90 to 400 K. Precise control of both flowrate and pressure is provided by dual precision metering pumps. Details are presented on a new calorimeter which incorporates several innovations. Heat losses from this calorimeter are reduced by a novel shielding arrangement and were shown to be less than the experimental precision of ±0.1 per cent. The calorimeter can be operated in either the isobaric or the throttling mode. The results of experimental determinations around the critical point of ethane are described. Enthalpies of vaporization and heat capacities were obtained by operating in the isobaric mode. Determinations in the throttling mode yielded isothermal throttling coefficients and Joule–Thomson coefficients. Analysis of these results showed that the thermodynamic consistency of the enthalpies in the isobaric and isothermal mode is better than 0.1 per cent, and that of the derived values of properties is 0.4 per cent or better.

1. Introduction

Accurate values of the physical properties of fluids are essential for designing energy-efficient process equipment. Of 'particular importance are the thermodynamic properties: enthalpy, heat capacity, and the throttling coefficients. In recognition of this need, extensive direct calorimetric determinations of the effect of pressure and temperature on the enthalpy of pure compounds and mixtures over a wide range of conditions have been carried out at the Thermal Properties of Fluids Laboratory, as reviewed in detail elsewhere.[1] These results were obtained on a recycle flow facility which had been developed over the past 20 years.

By building on this past experience and incorporating new ideas, it was reasoned that an entirely new recycle-flow facility might be built which would not only yield results of improved accuracy but which would also prove to be considerably easier to control and operate. The purposes of this paper are to describe such a facility and to present calorimetric results obtained with ethane near its critical point.

Details of the bases of flow calorimetry and the interpretation of results obtained on such facilities have been presented elsewhere.[2] In brief, fluid of constant

---

[a] Presently with Asahi Chemical Industry Co., Tokyo, Japan.

composition x flows through a calorimeter under steady-state conditions. When the calorimeter is properly designed and operated, both kinetic and potential effects are negligible and the calorimeter is, to all intents and purposes, adiabatic. Measured quantities of electric power P may be transferred to the fluid in the calorimeter during the course of the experiment. Under these constraints, the first law of thermodynamics reduces to

$$h(T_o, p_o) - h(T_i, p_i) = -P/F, \tag{1}$$

where the subscripts o and i serve to identify the state (temperature and pressure) at the outlet and inlet of the flow calorimeter and F denotes the mass flow rate.

In isobaric determinations, $p_o \approx p_i$, and electric power serves to increase the temperature—or to bring about a phase change. In the throttling mode, $p_o \ll p_i$, in which case: $P = 0$ for Joule–Thomson experiments, or $t_o \approx t_i$ for isothermal (Eucken) determinations.

2. Equipment

The new apparatus was designed to improve upon the performance of the old in key ways: by yielding results of higher precision, by easier operation and over a wider range of conditions, and by requiring less working fluid. These objectives were attained by complementary achievements in two principal areas: the development of a single calorimeter capable of accurate results in both the isobaric and throttling modes; and the employment of superior methods for control and measurement of flow and of pressure of the working fluid. These two capabilities were integrated into a suitably designed well instrumented apparatus. A description of the most important features of all of these items follows, with details presented elsewhere.[3]
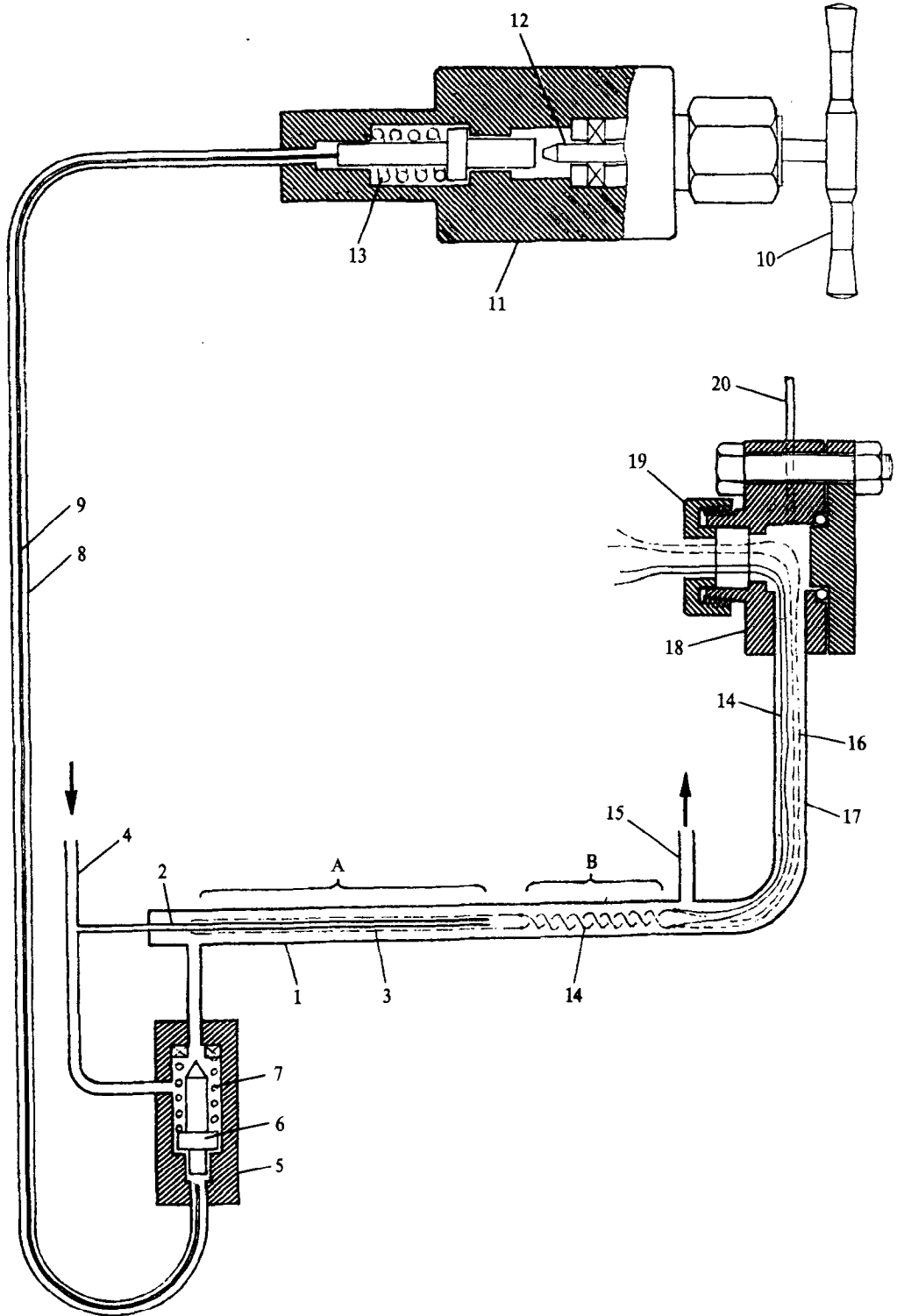
CALORIMETER

The key criteria selected in designing the new calorimeter were (a) to incorporate capability for isobaric and throttling determinations in a single calorimeter (both operation and instrumentation are simpler with one rather than two or more calorimeters); (b) to eliminate pressure seals at calorimeter operating temperatures, so that no pressure leaks will result from thermal expansion effects caused by varying calorimeter-bath temperatures; (c) to reduce heat losses to negligible values even at low flow rates; (d) to reduce the time to reach steady-state by reducing the mass of the calorimeter; (e) to achieve a basic design which will permit operation at pressures up to 100 MPa over a wide range of temperatures. The following description of the calorimeter illustrates briefly how each of these key criteria were satisfied.

FIGURE 1. Schematic diagram illustrating the technique used in incorporating both isobaric and throttling capabilities in a single calorimeter. 1, 4.76 mm o.d. tubing; 2, 0.07 cm i.d. capillary tubing; 3, electric heating wire; 4, 3.18 mm o.d. tubing; 5, shut-off valve; 6, plunger; 7, spring; 8, 1.58 mm o.d. tubing; 9, 0.5 mm piano wire; 10, turning handle; 11, wire adjuster; 12, stem; 13, spring; 14, electric heater lead; 15, 3.18 mm o.d. tubing; 16, electric-potential measurements tap; 17, 4.76 mm o.d. tubing; 18, lead wire seal unit; 19, wire seal fitting; 20, pressure tap; A, heating zone; B, mixing zone.

The technique used in incorporating both isobaric and throttling in a single calorimeter is illustrated schematically in figure 1. This is achieved using concentric tubes 1 and 2 in the heating section A, together with a small externally-activated self-sealing shut-off valve 5. The outer tube 1 is 4.75 mm o.d. The capillary inner tube 2 (0.07 cm i.d.) is wrapped with heating wire 3. When the valve 5 is open (as shown), fluid flows through both tubes 1 and 2 and the pressure drop is low (≈ 0.0005 MPa) yielding effectively isobaric determinations. With the valve closed, the entire flow is forced through the capillary, resulting in a high pressure drop, thus yielding throttling (isothermal or isenthalpic) results. The valve is remotely activated by a valve handle assembly 11 through a piano wire 9.

After exiting from the heating section A the fluid is mixed in section B by flowing over twisted and stuffed heater lead wires 14 and then exits through tubing 15. The heater lead wires 16 are led out of a Conax gland 19 in gland assembly 18. The pressure at the calorimeter outlet is measured through tap 20.

As may be seen in figure 1, there are only two high-pressure seals in this entire unit: one on the valve handle assembly 11 and the other in the Conax gland 19. Both of these are outside the calorimeter and are maintained at ambient conditions as desired.

The actual configuration of the arrangement (illustrated schematically by figure 1) and its incorporation into the calorimeter itself is shown in figure 2. The inlet fluid passes the inlet-pressure tap junction P and inlet-thermometer well T1, before flushing the two concentric radiation shields R1 and R2. It then enters a T and valve 5 which directs the fluid through one or both of the concentric tubes in the heating section 6 as was illustrated in figure 1. After thorough mixing in the tubes downstream from the heating section, the fluid passes through a tube surrounding the outlet-thermometer well T2, and exits from the calorimeter through a coiled tube which was designed to reduce conductive heat transfer with the bath. The lead wires from the heater in 6 are led out through the calorimeter outlet-pressure tap 4 to a Conax gland (19 in figure 1).

Heat losses are reduced in several ways. Shields R1, R2, R3, and R4 reduce radiative heat transfer with the surroundings. The calorimeter assembly is insulated by a vacuum jacket 1. Finally, the lengths and diameters of all the tubing leading in and out of the calorimeter are designed to reduce conduction losses.

The calorimeter is constructed entirely from 3.18 mm and 4.76 mm tubing, which helps to satisfy the remaining criteria. Using welded tubing throughout rather than having high-pressure closure devices reduces the mass and hence improves the response time to changes in calorimeter conditions. A further advantage of small o.d. tubing is that the same basic design can be scaled up to high pressures by slight changes in wall thickness. Thus, though the present calorimeter is capable of operating only up to 20 MPa, the basic design can be used up to 100 MPa.

FLOW METERING

The wide range of operation and the exceptionally precise results obtainable on the present dual-purpose calorimeter are due primarily to the special precision-machined piston pumps, designed by the late Walter Ruska of Rice University. These two
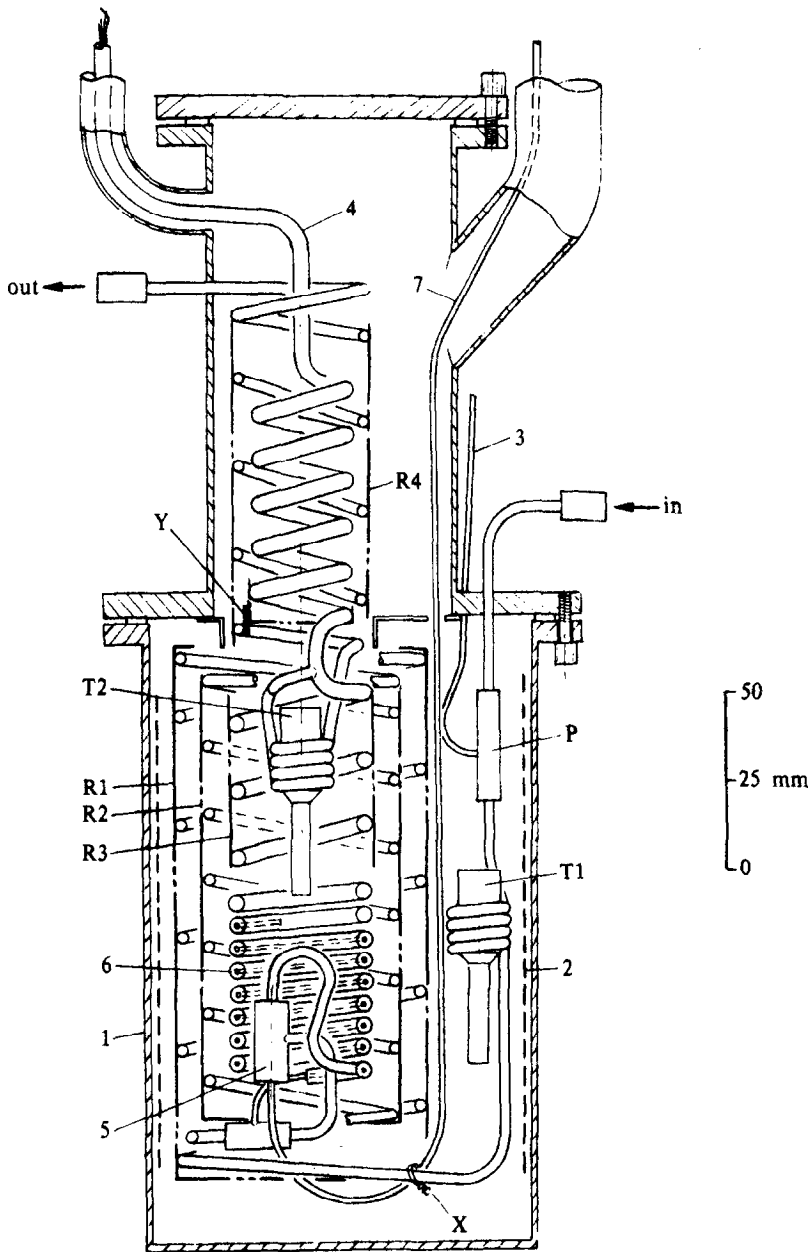
FIGURE 2. Schematic diagram of the calorimeter assembly. 1, Vacuum jacket; 2, guarded radiation shield; 3, calorimeter inlet-pressure tap; 4, calorimeter outlet-pressure tap; 5, shut-off valve; 6, calorimeter section; 7, piano-wire lead tubing; P, inlet-pressure tap junction; R1, radiation shield; R2, radiation shield; R3, radiation shield; R4, radiation shield; T1, inlet-thermometer well; T2, outlet-thermometer well; X, thermal contact; Y, thermal contact.

metering pumps, illustrated schematically (P-1A and P-1B) in figure 3, are driven through a gear assembly by a synchronous motor. They are designed to pump liquid at pressures up to 65 MPa at temperatures as low as 77 K. They deliver a volumetric flow constant to within 10^{-5}. After gravimetric calibration, the accuracy of the flow rate from these pumps is estimated to be ± 0.05 per cent. The volumetric flow rate of fluid is normally about 0.23 cm^3 s^{-1}, but can be altered by changing the drive gears.

AUXILIARY FACILITIES

The auxiliary facilities combine the calorimeter and flow-metering pumps into a recycle-flow system in which fluid flow is maintained at a constant rate through the calorimeter at a fixed predetermined pressure.

The scheme for maintaining unidirectionally continuous flow through the calorimeter is illustrated in figure 3. The pumps act in tandem, one receiving and the other discharging fluid. Four cryogenic solenoid-activated valves V1 to V4 and check valves operate in conjunction with the reversal motion of the pumps to provide unidirectional flow through the calorimeter.

Three sets of calibrated flexible-bellows pressure transducers F-11, F-12, and F-13 are important links for controlling and measuring the pressure. The pressure of the experimental fluid in this essentially constant-volume system is set approximately using bellows F-12 and handpump P-12. The desired pressure is set precisely in a thermostatted tank C-1 of helium and is measured by a Ruska 2400HL Dead-Weight Gauge through bellows F-13. The pressure of fluid is maintained essentially constant via bellows F-11 by a large helium buffer: tank C-1. This is especially important for smoothing out the slight disturbance in pressure which occurs following reversal of motion of the pumps. The value of the pressure at the calorimeter inlet is determined from the pressure in the tank C-1, the measured pressure difference across F-11, and the pressure drop of the fluid between F-11 and the calorimeter as measured by a transducer (LDPT in figure 3).

The metering pumps along with two sets of bellows F-11 and F-12, and the four cryogenic valves V1 to V4, are located in the pump bath B-1. For all the measurements reported here the temperature of this bath was 255.37 K so that ethane was always a liquid within the operating range of pressures (3 to 13 MPa). This liquid ethane is pumped through conditioning coils in the pre-conditioning bath B-2 and in the calorimeter bath B-3, before entering the calorimeter. Both the pre-conditioning and the calorimeter baths are maintained at the desired temperature of the experimental determinations. The post-conditioning bath which is held at 255.37 K serves to recondition the fluid to the temperature of the pump bath.

The temperature of the calorimeter bath is controlled to ± 0.02 K using a Hallikainen Thermotrol Model 1053 temperature controller. The pump bath temperature is held to ± 0.05 K using a similar Thermotrol Model 1109 temperature controller. A Bayley Model 121 temperature controller is used on the conditioning baths B-2 and B-4. Liquid nitrogen is the coolant for all the baths.
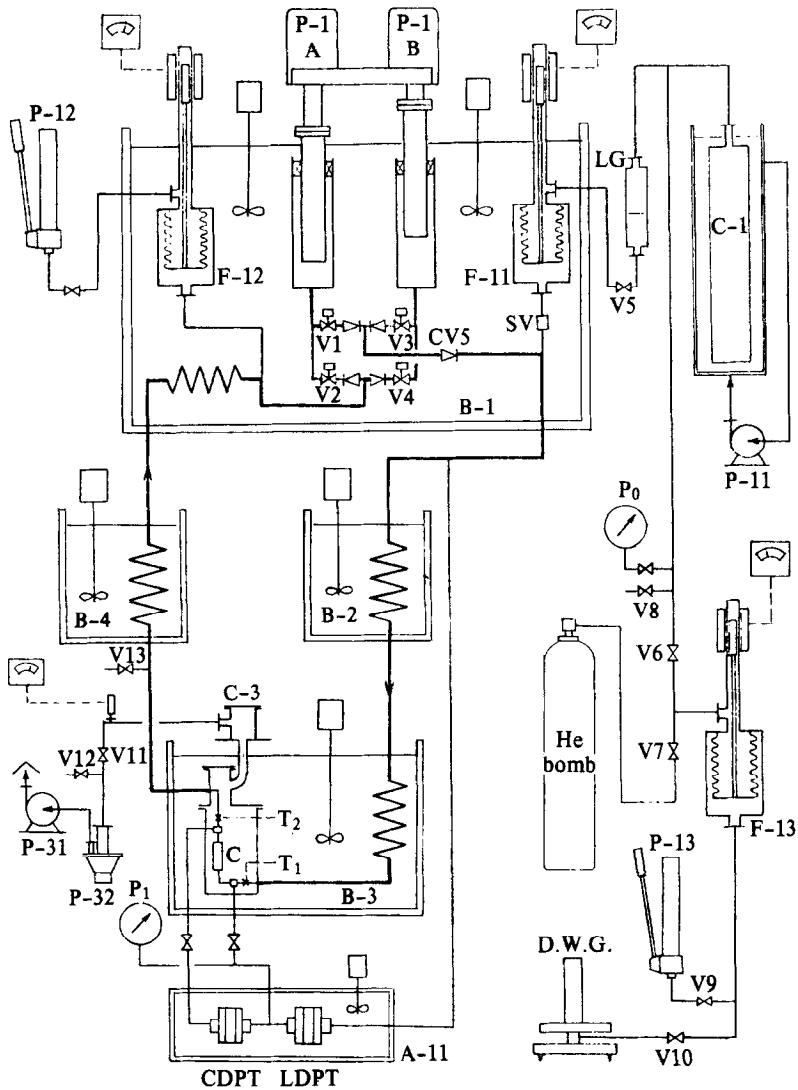
FIGURE 3. Schematic diagram of the recycle-flow calorimetric assembly. P-1A and P-1B, Metering pumps; —⋈—, solenoid valve; —◁|—, check valve; —⋈—, shut-off valve; B-1, pump bath; B-2, pre-conditioning bath; B-3, calorimeter bath; B-4, post-conditioning bath; A-11, air box; F-11, F-12, F-13, bellows; LG, level gage; P-12, P-13, oil pumps (manual); P-11, water circulation pump; P-31, vacuum pump; P-32, diffusion pump; P_1, P_o, Heise pressure gages; D.W.G., Ruska dead weight gage; C, calorimeter; C-3, calorimeter vacuum pot; CDPT, calorimeter differential pressure transducer; LDPT, line differential pressure transducer; SV, safety valve; T1, inlet thermometer; T2, outlet thermometer; C-1, helium cylinder; V1 to V4, solenoid operated on-off valves; V5 to V13, valves.

INSTRUMENTATION AND CALIBRATION

The prime measurements are power, pressures, temperatures, and flowrate. The actual instruments used and their capabilities are listed in table 1.

Power is supplied to the calorimeter by a Kepco power supply and is measured using a standard resistor circuit which is described in detail elsewhere.[2,3] All measurements of d.c. potential are made with a Leeds and Northrup K-5 potentiometer and 9828 null detector.

The temperatures of the fluid at the calorimeter inlet and outlet are measured by inserting the two probes of a Hewlett-Packard Quartz Crystal Thermometer into thermometer wells T1 and T2 respectively (figure 2). A redundant measurement of the temperature difference is provided by a 6-junction thermopile. In this work the temperature of the inlet fluid was assumed to be that measured by the quartz probe at T1. This temperature agreed with the bath temperature measured by the platinum resistance thermometer within the combined uncertainties (± 0.02 K) of the two instruments. The calorimeter outlet temperature was calculated from the inlet temperature of the fluid and the temperature difference measured by the thermopile, which agreed (± 0.02 K) with the temperature measured by the quartz probe at T2.

Initially, mass flowrates delivered by the pump were calculated from available volumetric data on ethane.[4] However, gravimetric calibration of the pumps as a

TABLE 1. Calibration and accuracy of key instrumentation used for calorimetric determinations

Variable	Instrument	Calibration	Estimated accuracy
Power input	1. Kepco PVS 100-IMG d.c. power supply	—	
	2. Standard resistors	N.B.S.[a]	0.03 per cent
	3. Leeds & Northrup K-5 Potentiometer and 9828 Null Detector	—	
Calorimeter inlet pressure	1. Ruska 2400HL oil dead-weight gauge	N.B.S.[a]	
	2. F-11 bellows transducer[b]	In house	0.0007 MPa
	3. BLH transducer Type HLD, Model 1300	In house	
Calorimeter pressure drop	1. Sensotec transducer, Model ZD	In house	
Calorimeter inlet temperature	1. Platinum resistance thermometer for calorimeter bath, Rosemount Model 162C	N.B.S.[a]	0.003 K in present temperature range
	2. Quartz crystal thermometer Hewlett-Packard Model 2801A	Hewlett-Packard	± 0.02 K
Calorimeter outlet temperature	1. Quartz crystal thermometer	Hewlett-Packard	± 0.02 K
Temperature difference between calorimeter inlet and outlet	1. 6-junction thermopile	N.B.S.[a]	± 0.002 K
Flowrate	Metering pumps	In house	± 0.05 per cent

[a] Traceable to N.B.S. [b] See figure 4.

function of pressure showed our measured densities to be uniformly higher by 0.45 per cent than the reported values. The gravimetric calibrations were used to calculate all mass flowrates because they represent a primary calibration. The calorimetric results reported in the thesis[3] are based on the volumetric determinations and therefore deviate uniformly by about 0.45 per cent from those reported here.

PROCEDURES

All bath temperatures are fixed at the desired level. The calorimeter valve, 11 in figure 1, is set for either isobaric or throttling mode. The system pressure is set approximately using pump P-12 and bellows F-12, with valve V-5 closed (see figure 3). The pressure in the helium ballast tank C-1 is adjusted to the desired level and valve V-5 is opened, allowing control of the system pressure via bellows F-11. Flow and power are established and the pressure readjusted precisely. This procedure is rapid, and the elapsed time from startup to recording the first point is 90 min or less.

In the isobaric mode the power supplied to the calorimeter is increased step-wise, and the corresponding step increases of temperature at the calorimeter outlet are noted after steady-state is attained. By reducing these results, the enthalpy difference across the calorimeter corresponding to each outlet temperature measurement is obtained, which may then be interpreted to yield the specific enthalpy of vaporization Δh_v or isobaric specific heat capacity:[3]

$$c_p = (\partial h/\partial T)_p. \tag{2}$$

In the throttling mode, if the fluid in the calorimeter cools on expansion, electric power is supplied to equalize the calorimeter inlet and outlet temperatures to within about 0.02 K. This type of measurement is repeated at several pressures. The effect of pressure on the isothermal throttling coefficient:

$$\phi = (\partial h/\partial p)_T, \tag{3}$$

may be obtained from these results.[3]

An isenthalpic determination can be made if no power is supplied to the calorimeter heater and the Joule–Thomson coefficient μ_{JT} may be directly obtained:[3]

$$\mu_{JT} = (\partial T/\partial p)_h. \tag{4}$$

The time required to make any one of these determinations ranges from 15 to 30 min, depending on whether there is high- or low-density fluid in the calorimeter. This time is less than the 40 min between reversals of the pump at normal flow rates.

4. Experimental results and their interpretation

The objectives of the experiments were (a) to obtain better results to test the performance of the equipment, and (b) to better define the thermodynamic properties of ethane in the important critical region. Hence, isobaric and throttling
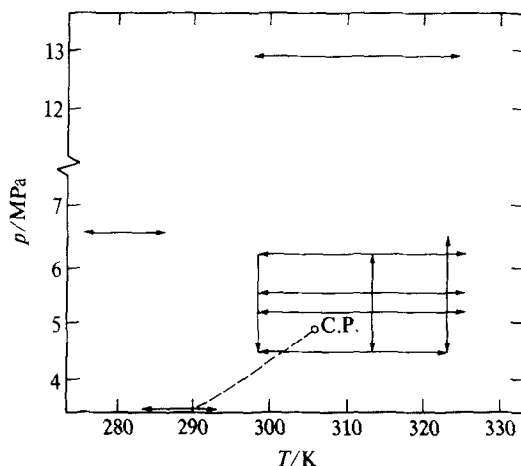
FIGURE 4. Range of calorimetric determinations on ethane.

determinations were made with ethane (99.7 moles per cent C_2H_6, 0.3 moles per cent C_3H_6) in the vicinity of the critical point, as represented schematically in figure 4. The enthalpies from these determinations were interpreted to yield values of the enthalpy of vaporization, heat capacities, isothermal throttling coefficients, and Joule–Thomson coefficients. These values also provided several important checks of thermodynamic consistency.

MEASUREMENTS IN THE ISOBARIC MODE

Determinations were made which yielded enthalpies of vaporization in the two-phase region and heat capacities near the critical point. The experimental results for all isobaric determinations are listed in table 2. When operating in this mode there is a small operational pressure difference across the calorimeter (Δp in column 3). In order to obtain the true isobaric enthalpy difference Δh it is necessary to apply a small correction $\delta \Delta h$ to the ratio of power to flow P/F.

The determination of the enthalpy of vaporization at a temperature about 4 K below the critical temperature is illustrated in figure 5. Ethane enters the calorimeter as a liquid, and the outlet temperature rises with increasing power input until two phases appear in the calorimeter. The outlet temperature remains relatively constant until all the liquid has vaporized and then rises again with increasing power input. The appearance and disappearance of two phases in the calorimeter is marked by breaks from which the enthalpy of vaporization may be determined.

There is an approximately 0.1 K rise in temperature across the two-phase region at a fixed pressure (figure 5). This is probably due to the 0.3 moles per cent of C_3H_6. The measured enthalpy of vaporization and the temperature of liquid-vapor coexistence at 3.444 and 4.473 MPa are listed in table 3.

The results of this work are compared in figure 6 with enthalpies of vaporization reported by Furtado[5] and Douslin and Harrison.[6] There is good agreement

TABLE 2. Experimental isobaric results for ethane

Run no.	p_i MPa	Δp MPa	T_i K	T_o K	P W	F g s^{-1}	$\delta\Delta h$ J g^{-1}	Δh J g^{-1}
1	4.4733	0	298.460	300.039	1.1966	0.10344	−0.004	11.564
2	4.4719	−0.0003	298.446	300.987	2.1274	0.10344	−0.004	20.562
3	4.4733	−0.0003	298.459	301.181	2.3516	0.10344	−0.004	22.730
4	4.4733	−0.0003	298.456	301.261	2.6001	0.10344	−0.004	25.132
5	4.4733	−0.0001	298.455	301.298	2.9373	0.10344	0	28.396
6	4.4726	0.0005	298.456	301.296	3.3241	0.10344	0	32.135
7	4.4726	0.0006	298.455	301.302	4.7866	0.10344	0	46.274
8	4.4726	0.0006	298.457	301.327	6.5152	0.10344	0	62.984
9	4.4726	0.0006	298.459	301.309	7.4791	0.10344	0	72.303
10	4.4726	0	298.457	301.324	8.0885	0.10344	0	78.194
11	4.4726	0	298.457	301.330	9.3806	0.10344	0	90.685
12	4.4726	0	298.455	301.348	10.7683	0.10344	0	104.10
13	4.4733	0	298.462	301.375	13.2938	0.10344	0	128.51
14	4.4726	0	298.445	301.874	17.5802	0.10344	0	169.95
15	4.4726	0.0007	298.451	303.276	19.1420	0.10344	0	185.05
16	4.4726	0	298.450	305.510	20.7683	0.10344	0	200.77
17	4.4740	0.0004	302.506	305.021	2.1270	0.10344	0.025	20.587
18	4.4740	0.0004	302.509	309.950	4.7839	0.10344	0.021	46.269
19	4.4740	0.0005	302.502	319.227	8.4992	0.10344	0.017	82.181
20	4.4740	0.0005	302.510	323.836	10.0675	0.10344	0.017	97.342
21	4.4740	−0.0010	320.884	324.549	1.1948	0.10002	−0.038	11.908
22	5.1699	−0.0003	298.456	302.085	2.1276	0.10407	−0.004	20.440
23	5.1669	0	298.462	303.750	3.3241	0.10407	0	31.942
24	5.1669	−0.0003	298.470	305.405	4.7858	0.10407	−0.013	45.975
25	5.1669	0	298.470	306.733	6.5132	0.10407	0	62.587
26	5.1676	0	298.459	307.576	8.5048	0.10407	0	81.724
27	5.1676	0	298.462	308.332	13.2859	0.10407	0	127.66
28	5.1676	−0.0001	298.468	309.267	16.0741	0.10407	−0.025	154.43
29	5.1676	0	298.471	311.249	19.1268	0.10407	0	183.79
30	5.1676	0	298.469	315.383	22.4417	0.10407	0	215.64
31	5.1662	−0.0006	313.169	318.412	3.3198	0.10407	−0.033	31.867
32	5.1662	0	313.178	321.364	4.7790	0.10407	0	45.925
33	5.1662	0	313.178	325.442	6.5034	0.10407	0	62.493
34	5.5144	−0.0003	298.467	302.409	2.1274	0.10439	−0.004	20.375
35	5.5137	0	298.478	306.323	4.7854	0.10439	0	45.841
36	5.5144	−0.0002	298.475	309.650	8.5042	0.10439	−0.008	81.456
37	5.5144	0	298.481	310.704	10.7617	0.10439	0	103.09
38	5.5144	0	298.485	311.396	12.7579	0.10439	0	122.21
39	5.5144	0	298.485	312.725	16.0714	0.10439	0	153.95
40	5.5144	0	298.472	314.768	19.1240	0.10439	0	183.19
41	5.5158	−0.0005	313.162	315.624	3.3205	0.10439	−0.059	31.749
42	5.5158	0	313.167	319.705	6.5060	0.10439	0	62.323
43	5.5158	0	313.172	323.190	8.4949	0.10439	0	81.375
44	5.5117	0	310.171	311.341	2.7901	0.10094	0	27.643
45	5.5117	−0.0005	310.174	312.211	5.3126	0.10094	−0.126	52.508
46	6.2025	−0.0004	298.487	302.899	2.1277	0.10500	−0.004	20.260
47	6.2025	0	298.489	307.619	4.7854	0.10500	0	45.577
48	6.2025	−0.0003	298.488	312.614	8.5034	0.10500	−0.012	80.974
49	6.2025	0	298.495	316.587	13.2811	0.10500	0	126.49
50	6.2025	0	298.496	318.507	16.0668	0.10500	0	153.02
51	6.2025	−0.0004	298.499	320.995	19.1282	0.10500	−0.042	182.13
52	6.2025	0	298.497	323.290	21.2746	0.10500	0	202.62
53	6.1067	−0.0003	297.709	303.637	2.1276	0.10978	0	19.381
54	6.1067	−0.0003	297.706	310.758	4.7850	0.10978	0	43.588

TABLE 2—continued

Run no.	$\dfrac{p_i}{\text{MPa}}$	$\dfrac{\Delta p}{\text{MPa}}$	$\dfrac{T_i}{\text{K}}$	$\dfrac{T_o}{\text{K}}$	$\dfrac{P}{\text{W}}$	$\dfrac{F}{\text{g s}^{-1}}$	$\dfrac{\delta\Delta h}{\text{J g}^{-1}}$	$\dfrac{\Delta h}{\text{J g}^{-1}}$
55	6.1067	−0.0003	297.707	320.304	8.5007	0.10978	0	77.436
56	6.1053	0	297.739	325.910	10.7747	0.10978	0	98.150
57	6.5390	−0.0003	275.215	287.229	4.1784	0.10271	0	40.682
58	6.5376	−0.0002	275.220	287.267	3.5480	0.08691	0	40.826
59	6.5397	0	275.226	287.241	1.9439	0.04780	0	40.670
60	6.5383	−0.0004	275.215	287.244	5.1220	0.12553	−0.004	40.799
61	3.4439	0.0002	283.178	285.328	0.9008	0.09892	0	9.107
62	3.4439	0	283.172	287.588	1.9245	0.09892	0	19.456
63	3.4439	0	283.171	288.490	2.3505	0.09892	0	23.762
64	3.4439	0	283.191	289.019	2.5809	0.09892	0	26.092
65	3.4446	0.0005	283.182	289.109	2.8207	0.09892	0	28.516
66	3.4439	0	283.175	288.972	3.0707	0.09892	0	31.043
67	3.4432	0	283.176	288.968	3.3320	0.09892	0	33.685
68	3.4446	0	283.165	289.032	6.1621	0.09892	0	62.296
69	3.4439	0	283.178	289.077	12.5983	0.09892	0	127.36
70	3.4446	0	283.165	289.133	21.8266	0.09892	0	220.65
71	3.4446	0	283.167	289.486	23.7246	0.09892	0	239.84
72	3.4439	0	283.173	289.525	24.9294	0.09892	0	252.02
73	3.4439	0	283.171	290.407	26.4073	0.09892	0	266.96
74	3.4439	0	283.177	294.209	27.9235	0.09892	0	282.29
75	3.4439	0.0015	283.175	296.718	28.6987	0.09892	0	290.13

TABLE 3. Specific enthalpies of vaporization Δh_v at given temperatures and pressures for ethane

p/MPa	T/K	$\Delta h_v/\text{J g}^{-1}$
4.473	301.35	138
3.444	289.05	234

between values shown in figure 6 but the enthalpies of vaporization reported here agree more closely with the values of Furtado than those of Douslin and Harrison. The composition of the ethane used by Furtado was very similar to that used in this work with the primary impurity being C_3H_6 (0.3 to 0.4 mole per cent) whereas Douslin and Harrison's sample contained fewer impurities. Propene is denser than ethane so the enthalpies of vaporization reported here and by Furtado agree more closely and are slightly higher than those given by Douslin and Harrison.

Specific heat capacities c_p are obtained by interpreting the results of isobaric determinations in the single-phase region. Typical results at 5.514 MPa are shown in figure 7. Mean values of c_p, determined both from direct measurements (solid horizontal lines) and by differencing experimental results (dashed horizontal lines), are plotted against temperature. Point values of c_p are obtained by a trial-and-error determination of an equal area curve through the mean c_p values as indicated by the solid curved line. Values of c_p at selected values of temperatures obtained in this manner are presented in table 4.
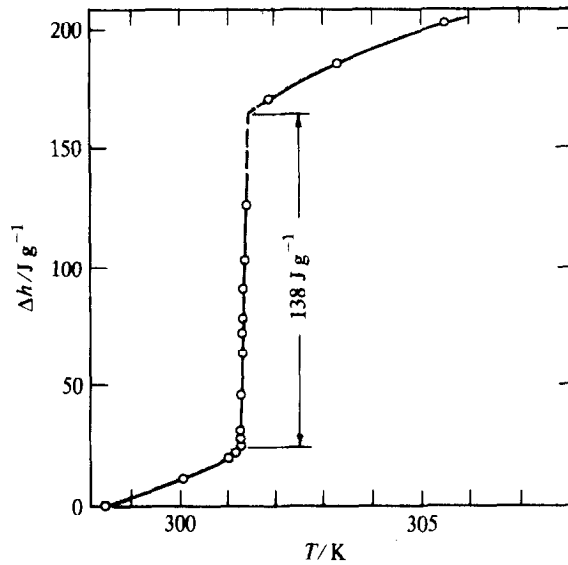
FIGURE 5. Isobaric traverse across two-phase region for the determination of the enthalpy of vaporization of ethane at 4.473 MPa.
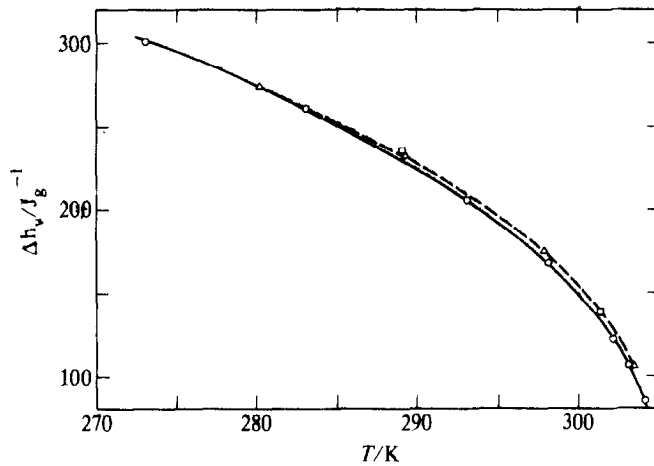

FIGURE 6. Enthalpy of vaporization Δh_v of ethane. ———, $\bigcirc$, Douslin and Harrison;[6] $\square$, present results; – – –, $\triangle$, Furtado.[5]

The variation of heat capacity with temperature at several pressures is shown in figure 8. At a pressure of 5.167 MPa, less than 0.3 MPa above the critical point, a sharp peak of magnitude 15 times "normal" values is encountered.

Our heat capacities are compared in figure 8 with values calculated by Goodwin, Roder, and Straty.[7] There is good agreement within their and our combined accuracies.
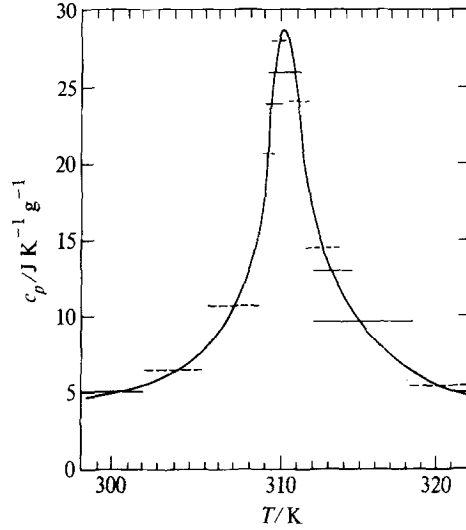
FIGURE 7. Isobaric heat capacity of ethane at 5.514 MPa.
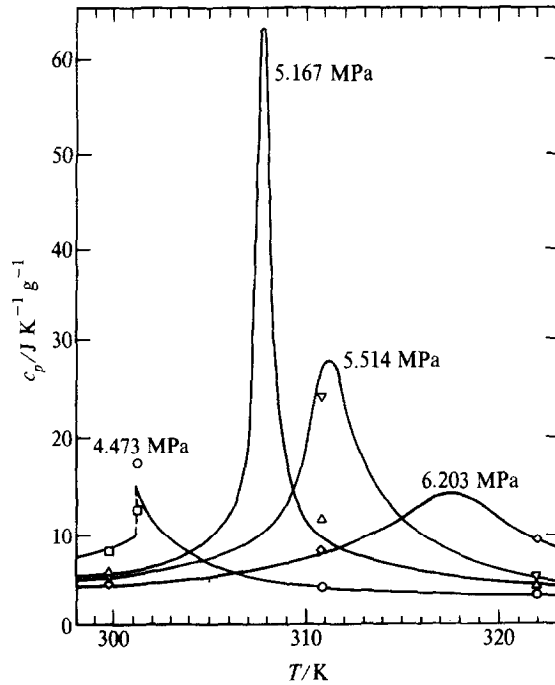
FIGURE 8. Smoothed specific heat capacities of ethane at four pressures shown as solid curves. Comparison with values of Goodwin et al.[7] $\bigcirc$, 4.473 MPa, liquid phase; $\square$, 4.743 MPa, vapor phase; $\triangle$, 5.167 MPa; ∇, 5.514 MPa; $\diamondsuit$, 6.203 MPa.

TABLE 4. Interpreted isobaric specific heat capacities

p/MPa:	4.473	5.167	5.514	6.203	13.001
T/K			c_p/J K^{-1} g^{-1}		
298.15	7.24	5.06	4.77	4.39	3.230
303.15	9.25	7.11	5.90	4.85	3.234
308.15	4.94	51.0	11.1	6.11	3.41
313.15	3.97	7.70	16.3	9.71	3.51
318.15	3.50	5.25	7.41	13.7	3.60
323.15	3.23	4.05	4.90	7.99	3.72

(In the vicinity of the maximum)

$p = 5.167$ MPa

T/K	307.15	307.55	307.95	308.55	309.15
c_p/J K^{-1} g^{-1}	23.4	38.9	63.2	31.0	14.6

$p = 5.514$ MPa

T/K	309.15	310.15	311.25	312.15	315.15
c_p/J K^{-1} g^{-1}	14.6	18.8	28.9	22.8	11.3

$p = 6.203$ MPa

T/K	315.15	316.55	317.45	318.15	320.15
c_p/J K^{-1} g^{-1}	12.1	13.6	14.0	13.8	11.4

MEASUREMENTS IN THE THROTTLING MODE

For the present determinations, the pressure drop varied from about 0.07 MPa for measurements in the liquid phase to about 0.2 MPa in the low-density vapor. The enthalpies from these determinations are given in table 5. In the throttling mode, the calorimeter was operated at nearly isothermal conditions. The small operational temperature difference ΔT across the calorimeter and the required correction $\delta\Delta h$ for non-isothermal conditions are listed in table 5. This correction is applied to the ratio P/F to obtain the true isothermal enthalpy difference Δh. Adiabatic measurements of Joule–Thomson coefficients were made by omitting power to the calorimeter.

Isothermal throttling coefficients were determined at several temperatures over a range of pressures as shown in figure 9. Since the measurements were made with a finite pressure drop across the calorimeter, it was necessary to interpret them to obtain values of ϕ. This is illustrated for the results at 313.16 K in figure 9 where mean ϕ values obtained from the measured enthalpy differences and pressure drop are plotted as bars. Smoothed values of ϕ were obtained by fitting an equal-area curve to the mean ϕ values and are plotted as the solid line in figure 9. At this temperature, the isothermal throttling coefficient goes through a maximum, attaining a peak value of -203 J g^{-1} MPa^{-1} at 5.612 MPa. Smoothed values of ϕ as a function of pressure at two other temperatures are also shown in figure 9. Tabulated values obtained from these curves are given in table 6.

Adiabatic Joule–Thomson measurements were made over a limited range of conditions. The objective of the experiments was to take sufficient points to obtain an
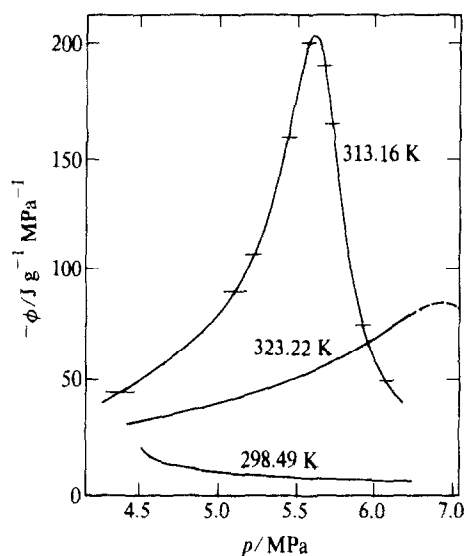
FIGURE 9. Isothermal throttling coefficients ϕ of ethane at 298.49, 313.16, and 323.22 K.

TABLE 5. Experimental isothermal results for ethane

Run no.	p_i MPa	Δp MPa	T_i K	ΔT K	P W	F $g\,s^{-1}$	$\delta\Delta h$ $J\,g^{-1}$	Δh $J\,g^{-1}$	$-\phi$ $J\,g^{-1}\,MPa^{-1}$
1	4.5843	0.0679	298.486	0.006	0.11738	0.10344	−0.0460	1.0887	16.031
2	5.2469	0.0665	298.485	−0.004	0.05962	0.10408	0.0209	0.5937	8.933
3	5.5241	0.0662	298.475	−0.012	0.04753	0.10436	0.0628	0.5182	7.830
4	6.1825	0.0658	298.483	−0.016	0.03196	0.10497	0.0628	0.3672	5.583
5	4.6195	0.1795	306.950	−0.003	1.36236	0.09997	0.013	13.639	75.972
6	4.8408	0.1505	306.954	−0.052	2.02738	0.10022	0.435	20.664	137.29
7	4.9573	0.1309	306.958	0.029	2.94705	0.09764	−0.301	29.881	228.34
8	5.0532	0.0969	306.959	0.041	7.05562	0.10047	−1.046	69.178	714.12
9	5.1766	0.0766	306.951	0.027	0.92722	0.10056	−0.7950	8.4260	109.99
10	5.3593	0.0720	306.949	0.008	0.34053	0.10072	−0.1004	3.2805	45.530
11	5.6682	0.0682	306.953	0.003	0.16097	0.10100	−0.0251	1.5686	23.004
12	6.1798	0.0669	306.913	0.005	0.10297	0.10139	−0.0335	0.9822	14.685
13	4.4761	0.2313	313.161	0.023	1.08633	0.10319	−0.088	10.439	45.129
14	5.1724	0.1645	313.163	0.019	1.41152	0.10398	−0.126	13.450	81.761
15	5.5158	0.1267	313.162	0.015	2.10362	0.10428	−0.221	19.951	157.52
16	5.7757	0.0967	313.172	0.004	1.66442	0.10453	−0.059	15.864	164.12
17	6.1108	0.0828	313.173	0	0.43978	0.10483	0	4.1951	50.662
18	5.3062	0.1409	313.155	−0.008	1.50124	0.10061	0.059	14.979	106.29
19	5.6447	0.1020	313.154	−0.001	2.04923	0.10094	0.017	20.317	199.24
20	5.7178	0.0940	313.166	−0.002	1.80040	0.10100	0.029	17.855	189.99
21	5.9709	0.0800	313.162	−0.028	0.57518	0.10133	0.3515	6.0276	75.365
22	4.6188	0.2359	323.219	0.020	0.81646	0.09992	−0.0653	8.1061	34.367
23	4.7284	0.2257	323.217	−0.010	0.80298	0.10003	0.0326	8.0602	35.717
24	5.1449	0.1948	323.215	−0.004	0.81611	0.10047	0.0209	8.1437	41.796
25	5.5448	0.1682	323.217	0.020	0.87004	0.10081	−0.1046	8.5263	50.682
26	5.9309	0.1428	323.208	−0.004	0.91130	0.10117	0.0293	9.0372	63.290
27	6.2073	0.1253	323.214	0.004	0.95349	0.10142	−0.0377	9.3640	74.746
28	6.3128	0.1174	323.218	0.008	0.95349	0.10153	−0.0753	9.3161	79.155
29	6.7493	0.0980	323.195	0.021	0.73557	0.10186	−0.2218	6.9996	71.392

TABLE 6. Interpreted values of the isothermal throttling coefficient

p/MPa	T/K: 298.49	313.16	323.22
	$-\phi$/J g^{-1} MPa^{-1}		
4.482	—	49.8	34.2
4.826	12.0	65.5	38.5
5.172	9.16	98.3	44.0
5.378	8.19	134	48.6
5.516	7.65	180	52.1
5.599	—	203	—
5.723	6.92	166	58.4
5.861	6.49	96.5	63.2
5.998	6.07	61.3	68.6
6.205	5.52	36.4	77.2

TABLE 7. Experimental Joule–Thomson coefficients

p_i/MPa	$-\Delta p$/MPa	T_i/K	$-\Delta T$/K	μ_{JT}/K MPa^{-1}
4.7029	0.2293	325.785	2.385	10.40
4.4746	0.2433	323.429	2.578	10.50
4.2306	0.2610	320.912	2.848	10.91
4.6064	0.2484	323.176	2.644	10.64
4.6085	0.2525	324.865	2.652	10.50
4.6091	0.2556	326.163	2.657	10.40

interpolated value of μ_{JT} at 323.22 K and 4.473 MPa in order to perform the thermodynamic-consistency check described later in this paper.

This check requires that the values of each of the three properties c_p, ϕ, and μ_{JT}, be obtained at the same conditions, 323.22 K and 4.473 MPa. The procedure for obtaining μ_{JT} was more complex than that for c_p and ϕ, which requires only interpretation of basic isobaric and isothermal results, as described earlier. It was necessary to make six isenthalpic determinations at pressures and temperatures about the desired conditions and the value of μ_{JT} was obtained by interpolation. The experimental results are listed in table 7.

5. Analysis of experimental results

The experimental results obtained were analysed to check on the performance of the equipment. A test was performed to determine if the heat leak in the calorimeter was less than experimental precision. Also, the isobaric and isothermal results were checked for internal self-consistency using thermodynamics.

CHECK ON THE ASSUMPTION OF ADIABATICITY

This check is essential since the calorimeter is designed to operate adiabatically, and the interpretation of the results is based on this assumption. Based on a principle
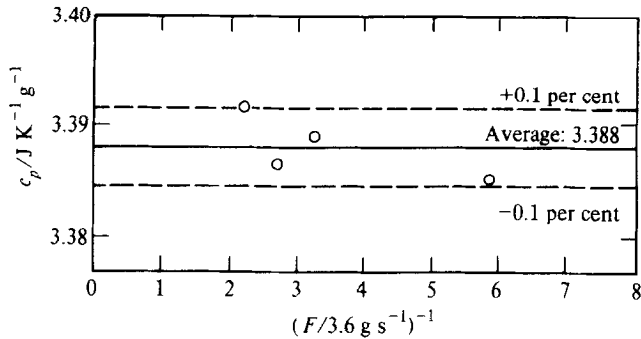
6

FIGURE 10. Mean heat capacity of ethane as a function of the reciprocal flow rate. Experimental conditions are $p = 6.537$ MPa, $T_i = 275.22$ K, and $T_o = 287.25$ K.

suggested by Montgomery and De Vries,[8] mean values of heat capacity were measured at fixed inlet and outlet temperatures and pressures over a range of flow rates to determine if such values are independent of flow rate. Results of measurements at 6.537 MPa (Runs 57 to 60 in table 2) are plotted in figure 10. The value of the measured mean heat capacity is independent of flow rate within the experimental precision of ± 0.1 per cent, justifying the assumption that the heat leaks from the calorimeter are negligible.

THERMODYNAMIC-CONSISTENCY CHECKS

The internal consistency of the results was tested in two ways: (a), by a loop check which sums isobaric and isothermal enthalpy differences around a closed loop in pressure and temperature; and (b), by a check on the mutual consistency of the point values of ϕ, c_p, and μ_{JT} at a fixed temperature and pressure.

Loop check. This check is based on the point property behavior of enthalpy where for a closed pressure and temperature loop, the sum of the enthalpy differences for a series of step changes in conditions is equal to zero. In practice, the experimentally determined enthalpy differences for the isobaric and isothermal measurements are summed and the deviation δ from zero is calculated:

$$\delta = \sum_{i=1}^{n} \Delta h_i \bigg/ \sum_{i=1}^{n} |\Delta h_i|, \qquad (5)$$

where Δh_i is the enthalpy change for the ith leg.

This is illustrated in figure 11 for a loop abcdefa which surrounds the critical point and traverses the two phase-region in the leg fa. This loop consists of two isothermal and three isobaric legs shown as solid lines. The dotted lines represent small corrections needed to close the loop.

The two isothermal enthalpy differences (ab and cd) were obtained by integrating the appropriate equal-area curves of ϕ against p from figure 9. In contrast, emphasis was placed on the direct experimental measurement of enthalpy in establishing the
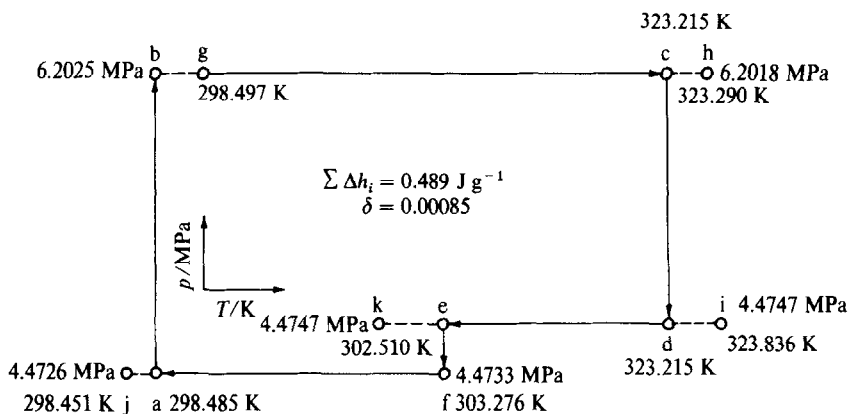
FIGURE 11. Loop for testing the thermodynamic consistency of isobaric and throttling results on ethane (see text).

isobaric legs. For determining the isobaric leg bc, an enthalpy difference of 202.614 J g^{-1} was obtained from run 52 (table 2) between 298.497 K and 323.29 K (leg gh). Corrections to 298.485 K (point b) and 323.215 K (point C) were calculated using smoothed values of c_p at these conditions and their values were $\Delta h_{bg} = 0.054$ J g^{-1} and $\Delta h_{ch} = 0.628$ J g^{-1}.

Results of two separate determinations (runs 15 and 20 of table 2) were used to obtain the enthalpy difference between points d and a. Four small corrections were needed to close the loop. Two of them, $\Delta h_{di} = 2.022$ J g^{-1} and $\Delta h_{aj} = -0.248$ J g^{-1} were made using smoothed values of c_p to obtain correspondence with the temperatures of the isothermal determinations. Two more corrections were needed to join e with f: (a), the enthalpy difference $\Delta h_{ek} = 7.602$ J g^{-1} between 302.510 K and 303.276 K was obtained by interpreting isobaric results from runs 13 through 15; (b), a value $\phi = -75$ J g^{-1} MPa^{-1} was estimated from isothermal determinations made at other temperatures and was used to calculate the enthalpy change from 4.4747 to 4.4733 MPa. The isothermal differences in enthalpy are $\Delta h_{ab} = -16.259$ J g^{-1} and $\Delta h_{cd} = 87.123$ J g^{-1}.

As indicated in figure 11, when all individual enthalpy differences are added around the closed loop, the result is 0.489 J g^{-1}. Expressed as a deviation, according to equation (5), the indicated thermodynamic consistency of the results is 0.085 per cent.

Thermodynamic identity check. The internal consistency of the interpreted values of the derivative properties obtained from isobaric, isothermal, and isenthalpic determinations can be checked by the identity:

$$\mu_{JT} = -\phi/c_p, \qquad (6)$$

At 323.22 K and 4.473 MPa, interpretation of isobaric and isothermal results yielded $c_p = 3.226$ J g^{-1} K^{-1} and $\phi = -34.04$ J g^{-1} MPa^{-1}. The calculated value of μ_{JT} obtained by substituting in equation (6) is 10.55 K MPa^{-1}. A value for the Joule–Thomson coefficient of 10.51 K MPa^{-1} at the same conditions (323.22 K and 4.473 MPa) was obtained by interpolation of the results from six measurements at temperatures and pressures around the desired values (table 7). Comparison of these

two values of μ_{JT} shows that the thermodynamic identity in equation (6) is satisfied to within 0.4 per cent.

PRECISION AND ACCURACY

The precision of the isobaric results appears to be about 0.1 per cent and that of the isothermal results about 0.5 per cent. Values of the derivative function estimated from these determinations are subject to errors in interpretation (especially where sharp maxima occur) but are consistent to about 0.4 per cent.

The accuracy of the results reported here is extremely difficult to estimate, especially in the regions close to the critical point where the thermodynamic properties change substantially with small variations in pressure and temperature. Comparisons with other independent experimental determinations would allow a good assessment of the accuracy. In the absence of such comparisons, it appears that the accuracy is about the same as the precision.

REFERENCES

1. Powers, J. E. *Advances in Cryogenic Engineering*, Volume 18. Timmerhaus, K.: editor. Plenum Press: New York. **1973.**
2. Yesavage, V. F.; Mather, A. E.; Katz, D. L.; Powers, J. E. *Ind. Eng. Chem.* **1967,** 59, No. IV, 35.
3. Miyazaki, T. M. Ph.D. Thesis, University of Michigan, Ann Arbor, Michigan. **1973.**
4. Pope, G. A. Ph.D. Thesis, Rice University, Houston, Texas. **1971.**
5. Furtado, A. W. Ph.D. Thesis, University of Michigan, Ann Arbor, Michigan. **1973.**
6. Douslin, D. R.; Harrison, R. H. *J. Chem. Thermodynamics* **1973,** 5, 491.
7. Goodwin, R. D.; Roder, H. M.; Straty, G. C. *Thermophysical Properties of Ethane from 90 to 600 K at Pressures to 700 bar*, Technical Note 684. U.S. National Bureau of Standards, Washington, D.C. **1976.**
8. Montgomery, J. B.; DeVries, J. *J. Am. Chem. Soc.* **1942,** 64, 2372.